Available online at www.sciencedirect.com

ScienceDirect

Procedia CIRP 27 (2015) 41 – 46

www.elsevier.com/locate/procedia

13th CIRP conference on Computer Aided Tolerancing

3D Measurement and Characterization of Ultra-precision Aspheric Surfaces

N. El-Hayek[a,b], N. Anwer[c,*], H. Nouira[b], O. Gibaru[a], M. Damak[a,d], P. Bourdet[c]

[a]*Arts et Métiers ParisTech, Laboratory of information sciences and systems (LSIS), 8 Boulevard Louis XIV, 59046 Lille, France*
[b]*Laboratoire Commun de Métrologie (LNE-CNAM), Laboratoire National de métrologie et d'Essais (LNE), 1 Rue Gaston Boissier, 75015 Paris, France*
[c]*ENS de Cachan, The University Research Laboratory in Automated Production, 61 avenue du Président Wilson, 94235 Cachan, France*
[d]*GEOMNIA, 165 Avenue de Bretagne, EuraTechnologies 59000 Lille, France*

* Corresponding author. Tel.: +33-(0)147402413; fax: +33-(0)14740220. *E-mail address:* anwer@lurpa.ens-cachan.fr

Abstract

Aspheric surfaces have become widely used in various fields ranging from imaging systems to energy and biomedical applications. Although many research works have been conducted to address their manufacturing and measurement, there are still challenges in form characterization of aspheric surfaces considering a large number of data points. This paper presents a comparative study of 3D measurement and form characterization of an aspheric lens using tactile and optical single scanning probing systems. The design of the LNE high precision profilometer, traceable to standard references is presented. The measured surfaces are obtained from the aforementioned system. They are characterized with large number of data points for which a suitable process chain is deployed. The form characterization of the aspheric surfaces is based on surface fitting techniques by comparing the measured surface with the design surface. A comparative study of registration methods and non-linear Orthogonal Least-Squares fitting Methods is presented. Experimental results are analyzed and discussed to illustrate the effectiveness of the proposed approaches.

Peer-review under responsibility of the organizing committee of 13th CIRP conference on Computer Aided Tolerancing
Keywords: Aspheric surface; form characterization; high precision metrology; non linear least-squares method; computational metrology

1. Introduction

Aspheric surfaces have become widely used in various applications such as optics, photonics and biomedicine. The manufacturing and measurement of such elements is still a common challenge in industry as the form characterization of aspheric surfaces is not yet normalized. This process becomes even harder when considering a large number of measurement points.

This paper presents a comparison of two measurement techniques and of three different fitting algorithms for the form characterization of aspheric surfaces. Optical and tactile single scanning probe systems are commonly used in dimensional metrology applications. However, in order to reach a nanometric level of accuracy in the measurement of aspheric lenses, ultra-high precision machines should be employed. Therefore, the design of the LNE's high precision profilometer, traceable to the SI meter definition is presented. Its architecture complies with the Abbe principle and its metrology loop is optimized. The performance and capability of the machine in the scope of aspheric lenses metrology are discussed.

The measured surfaces (MS) are obtained from the aforementioned system. They are characterized by a large number of data points (>100,000 points) which will be processed following a suitable procedure. The Design Surface (DS) of the aspheric lens can be described using different models. A conic-polynomial model which serves as a basis for aspheric lens specification, a discretized form of the polynomial into a set of reference points to create a nominal CAD form, and a mapping of that polynomial into a linear combination of orthogonal basis functions.

The form characterization of aspheric lenses is based on Orthogonal Least-Squares fitting techniques by comparing the measured surface with the design surface. A comparative study of an Iterative Closest Point (ICP) method and non-linear Orthogonal Least-Squares Optimization Methods is presented here. Three fitting algorithms are compared based on their capacities to converge quickly with an acceptable accuracy, to manage a large volume of data and to be robust

Peer-review under responsibility of the organizing committee of 13th CIRP conference on Computer Aided Tolerancing
doi:10.1016/j.procir.2015.04.041

and numerically stable. Experimental results are presented and discussed to illustrate the effectiveness of the proposed approaches.

2. LNE high precision profilometer

Measuring aspheric surfaces to an accuracy of few tens of nanometers remains an important challenge in manufacturing and metrology of freeform optics [1]. To achieve the best possible accuracies, specific ultra-high precision machines have been developed by the National Metrology Institutes (NMIs) that ensure the traceability chain. In this regard, a three-year project has been launched by the European Metrology Research Program (EMRP) [2] and encompasses a multitude of European National Metrology Institutes (LNE, PTB, VSL, METAS, SMD and CMI), industry and academia aiming at improving apparatus and methods for high-precision measurement of aspheric and freeform optics and characterizing their form. The apparatus are generally related to small-volume coordinate measuring machines that feature measuring ranges of hundreds of millimeters. These machines respect the Abbe principle, apply the dissociated metrological structure and incorporate high-precision mechanical guiding elements.

2.1. Description of the LNE high precision profilometer

LNE's high precision profilometer is a measurement machine (Fig. 1) capable of performing independent motions in all x, y and z directions using three independent high-precision mechanical guiding systems equipped with encoders. While x and y motions are controlled by sub-nanometer resolution laser interferometers, the z motion is controlled by a differential laser interferometer that allows to shorten the metrology loop and maintain a sub nanometric accuracy. Its working range in the xy-plane is 50×50 mm². The probe and its supporting structure are mounted on the vertical guiding system in the z-direction along which the measurement is done. The working range of the mechanical guiding system in z-direction is about 100 mm. The supporting frame is made of massive granite and carries the guiding elements. The metrology frame is made of Invar for minimal sensitivity to environmental influence.

The metrology loop incorporates three Renishaw® laser interferometers and is equipped either with a chromatic confocal probe or a tactile probe to achieve nanometric resolution measurement. The machine allows the in-situ calibration of the probes by means of the differential laser interferometer considered as a reference.

The uncertainty budget is established for the measurement of KNT4080-30 V-groove standards taking into consideration different and various error sources with the addition of the measuring probe's errors. The obtained results validate the capability of the profilometer to perform measurement on aspheric surfaces at the nanometer level of accuracy. The tactile and confocal measurements of the asphere take place in the LNE's cleanroom in which environmental conditions are optimal (temperature and humidity are controlled).

Then, the asphere is posed on the Zerodur table (Fig. 1) and is first measured by a tactile single point scanning probe which has been previously calibrated in-situ.

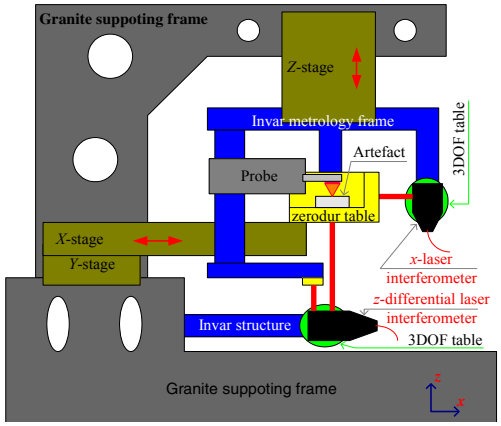

Fig. 1 Architecture of the LNE' high precision profilometer.

2.2. Evaluation of the LNE high precision profilometer

On this machine, it is not possible to exactly align the asphere's axis with the z axis of the measurement, however, an approximation of the apex position can be done by estimating the cusp of the surface. A large number of data points (>> 100,000 points) are recorded in the form of XY-grids (ranging from 5×5 mm² for confocal to 6×6 mm² for tactile). The optical probe's total measurement time is about half of the tactile probe's total measurement time since no contact needs to be established for the optical measurement.

3. Form characterization of aspheric surfaces

3.1. Mathematical representation of aspheric surfaces

The traditional way to represent aspheric surfaces is the axially symmetric quadric and power series parametric description as described in ISO 10110-Part 12 (Eq. 1)

$$z = \frac{cr^2}{1+\sqrt{1-(1+\kappa)\,c^2r^2}} + \sum_{j=1}^{m} \alpha_{2j} r^{2j}, \qquad (1)$$

where r is the radial coordinate, z is the sag (sagittal representation), c is the curvature at the apex, and κ is the conic constant. The $\alpha_{2j}r^{2j}$ terms are the higher order aspheric terms that represent the additive departure from the quadric.

Other mathematical formulations have been developed [3]. Among them orthogonal basis polynomials such as Q-polynomials and Zernike polynomials in an attempt to improve the classic power series and representing the useful surface shape with a small number of parameters. This makes each term unique and meaningful.

3.2. Aspheric surface fitting

The form evaluation of aspheres can be done by performing the fitting or association of the aspheric model to the measured data according to a criterion such as least-squares or minimum zone. The residuals of the fitting or the deviations to the associated reference model are then evaluated. The Peak-to-Valley (PV) and the Root Mean Square (RMS) are the most widely adopted parameters for the assessment of form deviations of aspheric surfaces.

Many fitting techniques are reported in the literature, but only few discuss the fitting of aspheres. Chen *et al* [4] propose an aspheric lens characterization by means of a 2D profile fitting. The dataset used is a profile measured using a stylus and the reference model is the corresponding asphere profile. The fitting is done using the Levenberg-Marquardt algorithm [5] for its quick convergence and precision. Similar works have been published and also deal with aspheric profile identification [6] and conic sections fitting [7]. Sun *et al* [8] perform fitting of aspheric curves and surfaces on simulated data with vertical distance minimization using a Gauss-Newton algorithm. In fact, they assume that the model and the data are both defined in the same reference frame. Other works involve approximating aspheres with NURBS models in order to generate CAD models for manufacturing purposes [9]. The problem of fitting the data to the aspheric surface model is posed as a nonlinear least-squares problem which is defined as follows (Eq. 2).

$$\min_{\lambda} \sum_{i=1}^{N} \left\| \mathbf{R}\ p_i + \mathbf{T} - q_i \right\|^2, \tag{2}$$

where λ is the set of shape, position and orientation variables, $\mathbf{R}$, $\mathbf{T}$ are transformation parameters, p_i is a data point, and q_i is the orthogonal projection of the data point p_i onto the reference model (footpoint). In this paper, position and orientation parameters as well as shape parameters are estimated. The process described here goes by optimizing for five transformation parameters, the symmetry about z axis is being redundant here. Two general approaches to solving this problem can be considered. In the sequential approach, algorithms are implemented in sequential computation of footpoints and transformation parameters. Unlike sequential approaches, the simultaneous approach can perform optimization of transformation parameters and footpoints simultaneously.

There exists vast literature about non-linear least squares fitting algorithms. Gauss-Newton type [10] and Levenberg-Marquardt (LM) type [11] have been recommended by NMIs. In this paper, we restrain the comparison to the sequential fitting implementation.

3.3. Orthogonal non-linear least squares fitting algorithms

The Newton-Raphson method [12] is used in this paper for the computation of orthogonal footpoints. The goodness of the approximation depends on the stop criterion and on the quality of the initial guess (relative position of the point data and the model should be close to the optimal solution) [12]. The vertical projection point is taken as an initial guess and the Newton-Raphson method iterates until the orthogonal projection point is accurately approximated.

Then for the objective function optimization, Levenberg-Marquardt (LM) can be used [5, 13]. LM is a well-known optimization algorithm that has been approved by the National Institute of Standards and Technology (NIST) for metrology applications that require fitting simple curves and surfaces in 3D [11]. Generally, this algorithm converges reasonably quickly and accurately for a wide range of initial guesses that are relatively close to the optimal solution [4]. However, the fitting of parametric curves and surfaces using the LM algorithm requires the calculation of a large Jacobian matrix and the storage of a considerable system of linear equations, as described by Speer *et al* [14].

For a very large number of variables or unconstrained non-linear problems, iterative quasi-Newton methods such as the Limited memory- Broyden-Fletcher-Goldfarb-Shanno (L-BFGS) method can be more convenient [15,16]. Like any minimization algorithm, L-BFGS preferably requires a twice differentiable objective function whose gradient must be zero at optimality. The advantage of this method is that it does not need calculating the inverse Hessian matrix of the objective function. It only approximates it using a limited amount of storage [15]: at every iteration, the inverse Hessian is approximated using information from the last m iterations with each time, the new approximation replacing the oldest one in the queue. L-BFGS is suitable for applications involving large volumes of data and variables [17].

3.4. Computational Geometry approaches

Computational geometry deals with the structure and complexity of discrete geometric objects as well as with the design of efficient computer algorithms for their manipulation. Registration and reconstruction are among the two most important research themes in computational geometry and can provide new research avenues to freeform surface fitting and Geometrical Product Specifications.

There exists various mesh reconstruction algorithms such as the Cocone algorithm which has been shown to fit the most our applications provided that a condition on the density of sampling is satisfied [18]. Another approach exploits the fact that aspherical surface datasets can generally be projected onto a plane following a bijective mapping without any superposition of points. The points are reconstructed in the plane using a 2D Delaunay triangulation which guarantees a correct mesh. Bijection offers the possibility of tracing back the points to their original positions without modifying the geometry and the topology of the underlying surface.

Meshes can serve as reference models when the problem needs to be expressed in discrete form. In this case, an Iterative Closest Point (ICP) optimization can be performed [19, 20]. Generally, ICP is used in registration operations but adaptations exist for its usage with mesh model cases. A mesh model offers the advantage of obtaining a more accurate distance calculation than a point model does. In general, d_{pm} (point-to-mesh distance) is smaller than d_{pp} (point-to-point distance).

4. Results and analysis

The comparison of the fitting algorithms is founded on two elements. Firstly, the effect of fitting data with orthogonal distance minimization is studied. Secondly, the effect of data size on the algorithms' complexity is analyzed and is based on two criteria, the units of memory used and the computational time expressed as Central Processing Unit time (CPU time). In order to vary the number of points in a dataset, no specific filtration technique is applied, but simply, points are sampled at different chosen rates.

The machine used for the tests is an Intel core i7/x64 platform with 8 Gb of RAM and a 2.0 GHz processor.

4.1. Simulated datasets

The aspherical model is simulated based on Eq. 1 by generating symmetrically distributed points around the asphere's axis (Fig. 2). Its design parameters have the following values ($c=10^{-20}$, $\kappa=-1$, $\alpha_2=0.02227$, $\alpha_4=7.29\times10^{-6}$, $\alpha_6=4.52\times10^{-9}$, $\alpha_8=-1.061\times10^{-11}$, $\alpha_{10}=9.887\times10^{-15}$).

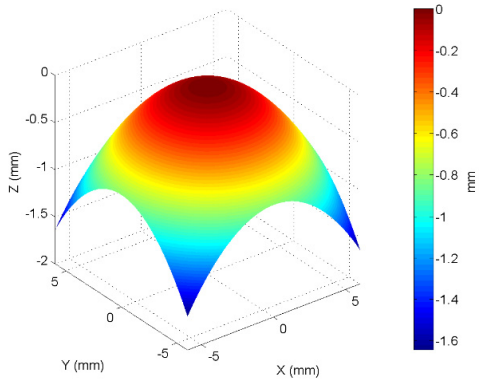

Fig. 2 Simulated asphere model without noise.

Then, simulations are performed in order to study the effect of data subject to errors both from measured object (form deviations) and measurement (Gaussian noise) [21]. Measurement errors simulation involves generating Gaussian noise with controlled mean and standard deviation. This value is coherent with noise that can manifest on the measurement sensors. A MATLAB random function is used to generate this noise which is added to the theoretical data in the orthogonal direction at each data point. Fractional Brownian Motion is also superimposed on the theoretical data in order to simulate form deviations [22]. The H parameter (Hurst index) is taken to be 0.9 and the span equal to the number of points in the simulated dataset [23].

The three fitting methods (LM, L-BFGS and ICP) are used to fit and analyze the data and the results are compared. The output transformation parameters of each algorithm as well as the model parameters that are computed after each fit are also compared. The RMS and PV values are also reported (Table 1). The RMS and PV of the simulated dataset are calculated upon generation and theoretically amount to 54.95 and 265.292 nm, respectively. From the results recorded in Table 1, all three algorithms are equivalent with respect to fitting. The transformation parameters are almost identical across L-BFGS, LM and ICP. Since ICP is only an algorithm for fitting two datasets geometrically, the model parameters cannot be estimated and the comparison in this matter restrains to L-BFGS and LM. The values of RMS and PV output by all three algorithms are very similar and are close to those of the simulated set.

Table1. Fitting using Least-Squares orthogonal distance minimization for the combined systematic and random errors (N: Number of points; t_p: transformation parameters; m_p: model parameters).

N = 500,000		L-BFGS	LM	ICP
t_p:	R_x (°)	-0.0086725	-0.0086463	-0.0086215
	R_y (°)	$1.853623E^{-4}$	$2.124006E^{-4}$	$1.96234E^{-4}$
	t_x (mm)	$7.276719E^{-5}$	$8.412097E^{-5}$	$-1.5734E^{-5}$
	t_y (mm)	0.0033001	0.0033197	0.0033952
	t_z (mm)	$-8.6709E^{-5}$	$-1.7561E^{-4}$	$-1.77180E^{-4}$
m_p:	c	$1.56046E^{-19}$	$1.0E^{-20}$	×
	κ	-1.0	-1.0	×
	α_2	0.02271712	0.0222847	×
	α_4	$7.293143E^{-6}$	$6.532301E^{-6}$	×
	α_6	$4.520966E^{-9}$	$2.68453E^{-8}$	×
	α_8	$-1.05786E^{-11}$	$-3.06699E^{-10}$	×
	α_{10}	$1.77676E^{-12}$	$1.44107E^{-12}$	×
RMS (nm)		51.68628	51.68615	51.6841
PV (nm)		236.2884	236.2927	236.3124

The fitted residual errors are slightly smaller than the theoretical values because there is a better position for the aspherical surface with respect to the generated Brownian motion errors. Overall, this part validates the algorithms used for the purpose of fitting aspherical data. Their accuracy is acceptable and is equivalent across all of L-BFGS, LM and ICP. For a theoretical dataset simulated without any added noise, fitting returns parameters that are identical to the design parameters; whereas in the case of added noise, these parameters present a slight variation (especially α_{10}).

4.2. Experimental data

The surface is first scanned using a tactile probe over an area of 6×6 mm², giving a grid of about 1,500,000 points. The results of the L-BFGS, LM and ICP fitting are detailed and compared for the experimental datasets for three different relative initial positions with respect to the reference model (Table 2). The first initial position (IP_1) is manually positioned to be very close to the model, IP_2 is shifted by few millimeters (+10 mm) in x and y directions, and IP_3 is the same as IP_1 but rotated with an angle of almost 90° about x.
Both L-BFGS and LM converge for all three cases, but ICP fails in the case of IP_3. The residual errors are identical at the nanometre level for all three algorithms and return a RMS value of 217 nm and PV of 2198 nm.

Table2. Fitting results of the tactile measurement for L-BFGS, LM and ICP algorithms.

N	L-BFGS *(nm)*		LM *(nm)*		ICP *(nm)*	
	RMS	PV	RMS	PV	RMS	PV
IP1						
75,000	217.18	2198.88	217.18	2198.39	217.22	2188.90
500,000	217.18	2198.84	217.18	2198.84	217.21	2189.59
1,500,000	217.18	2198.93	217.18	2198.93	217.21	2189.84
IP2						
75,000	217.19	2198.42	217.19	2198.42	217.22	2188.89
500,000	217.19	2198.87	217.19	2198.87	217.21	2189.92
1,500,000	217.19	2198.96	217.19	2198.96	217.21	2190.13
IP3						
75,000	217.18	2197.19	217.18	2197.19	×	×
500,000	217.18	2197.65	217.18	2197.65	×	×
1,500,000	217.18	2197.74	217.18	2197.73	×	×

In the same reference frame, the surface is then scanned using a chromatic confocal probe, giving a grid of about 5×5 mm² containing 1,000,000 points. For the same initial positions, IP_1, IP_2 and IP_3 of the dataset with respect to the model, and different dataset sizes, the fitting results are reported in Table 3.

Table3. Fitting results of the optical measurement for L-BFGS, LM and ICP algorithms; (*N*: Number of points).

N	L-BFGS *(nm)*		LM *(nm)*		ICP *(nm)*	
	RMS	PV	RMS	PV	RMS	PV
IP1						
50,000	336.40	6160.80	336.40	6160.73	336.41	6161.12
500,000	336.39	6156.95	336.40	6156.86	336.41	6157.61
1,000,000	336.39	6157.18	336.39	6157.16	336.41	6157.93
IP2						
50,000	336.40	6160.95	336.40	6161.03	336.41	6162.06
500,000	336.40	6157.06	336.40	6156.99	336.41	6158.12
1,000,000	336.39	6157.31	336.39	6157.26	336.41	6158.24
IP3						
50,000	336.40	6160.84	336.40	6160.94	×	×
500,000	336.40	6157.02	336.40	6157.13	×	×
1,000,000	336.40	6157.23	336.40	6157.38	×	×

The model parameters computed with the fitting of both the optical dataset or the tactile dataset are listed in Table 4. The experimental data show an equivalent accuracy among the two orthogonal distance-based fitting algorithms used which are also comparable to ICP in cases where the initial position of the elements to fit is relatively close (IP_1 and IP_2). Residual errors are illustrated in Fig. 3 for both tactile (Fig. 3a) and optical measurement fittings (Fig. 3b) using L-BFGS.

L-BFGS and LM perform faster than ICP in terms of computational time such as shown in Fig. 4. Although runtime is of the same order between LM and L-BFGS, the latter still performs a little faster than LM, and that, by a ratio of around 50%. For large volume datasets, the difference can be of some tens of seconds and therefore be critical for on-line metrology applications. Nevertheless, all three algorithms are very low on memory storage and datasets of several millions of points can be processed using any of these algorithms.

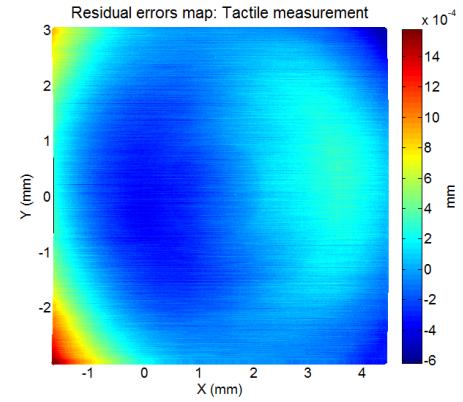

(a)

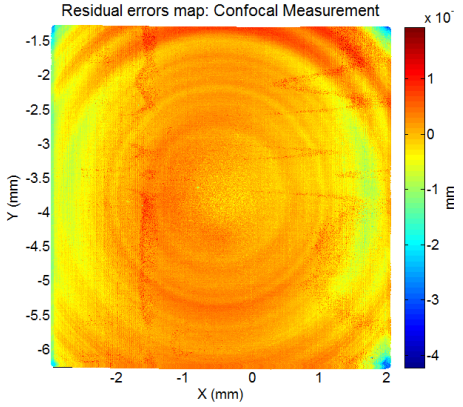

(b)

Fig. 3 Residual errors maps: (a) Tactile measurement fit, (b) Optical measurement fit.

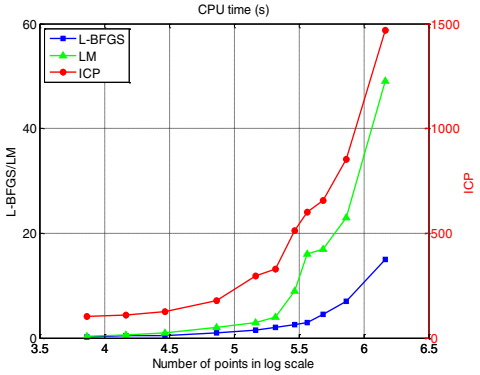

Fig. 4 CPU time performance of the L-BFGS, LM and ICP algorithms.

Table4. The model parameters of the asphere after fitting both the tactile and the confocal datasets.

N = 500,000		Tactile dataset	Confocal dataset
	R_x (°)	0.0022868	0.0109687
	R_y (°)	0.0057522	11.99958
t_p:	t_x (mm)	0.1286046	3.6542821
	t_y (mm)	-0.0510596	0.5042661
	t_z (mm)	-2.989905E^{-4}	-0.4847707
	c	4.969E^{-5}	2.192E^{-5}
	κ	-1.0	-1.0
	α_2	0.0223669	0.0223392
m_p:	α_4	-2.864146E^{-6}	-1.261943E^{-5}
	α_6	7.474612E^{-7}	1.27085E^{-6}
	α_8	-3.375417E^{-8}	-3.160791E^{-8}
	α_{10}	5.373977E^{-10}	2.737668E^{-10}

4.3. Discussions

L-BFGS, LM and ICP algorithms are tested on simulated datasets and they return similar results for the fitting on a given aspheric surface model. Since both algorithms are both Newtonian methods, applied on the same input datasets, it is logical that they converge to the same minimum. The algorithms are also tested on experimental datasets and the RMS and PV values are comparable. L-BFGS is slightly faster than LM and both perform faster than ICP. Nonetheless, all three algorithms are very low on memory storage and can thus process very large datasets. Furthermore, they return the same residual errors even if a subset of the points is considered. The adopted sampling strategy is that a reading is picked from the dataset but no filtration is applied. The Least-Squares minimization is not sensitive to point-set size when the latter has low uncertainty and contains a sufficient number of points. Tactile measurement is slower but more accurate than chromatic confocal measurement as the RMS and PV of the residual errors for tactile measurement are smaller, meaning that the tactile measurement is less noisy.

5. Conclusion and future work

This paper presents measurement and form characterization of aspheric surfaces. The comparison of optical and tactile measurements of an asphere using the LNE's high precision profilometer is done based on a surface form characterization. The performance and capability of the machine in the scope of aspheric lenses metrology are discussed. Simulations and experiments have been conducted to test and compare the performance of three different algorithms for aspheric surface fitting. The results show that L-BFGS performs better than LM and ICP in terms of computational time and is therefore more suitable for very large number of data points.

Future research efforts will concentrate on improving the robustness and accuracy of the L-BFGS algorithm. Reference data set generation for the validation of metrological software for the characterization of aspheric surfaces will be also investigated.

Acknowledgements

This work is part of EMRP Joint Research Project-IND10 "Optical and tactile metrology for absolute form characterization" project. The EMRP is jointly funded by the EMRP participating countries within EURAMET and the European Union.

References

[1] Fang, F., Zhang, X., Weckenmann, A., Zhang, G., Evans, C., 2013. Manufacturing and measurement of freeform optics, in "*CIRP Annals-Manufacturing Technology".*

[2] The EMRP website: http://www.emrponline.eu/

[3] Kaya, I., Thompson, K.P., Rolland, J.P., 2012. Comparative assessment of freeform polynomials as optical surface descriptions, in *"Opt. Express"*, Vol.20, pp. 22683–22691.

[4] Chen, Z., Guo, Z., Mi., Q., Yang. Z., Bai, R., 2009. Research of fitting algorithm for coefficients of rotational symmetry aspheric lens, in *Proc. SPIE 7283, 4th Intl. Symp. on Adv. Opt. Manuf. and Test. Tech.: Opt. Test and Meas. Tech. and Equip.,* Vol. 7283

[5] Moré, J., 1978. The Levenberg-Marquardt algorithm: implementation and theory, in "*Numerical analysis", Springer, pp. 105-116.*

[6] Aceves-Campos, H., 1998. Profile identification of aspheric lenses, in *"Applied Optics"*, Vol. 37 (34), pp. 8149-8150.

[7] Zhang, Z., 1997. A tutorial with application to conic fitting, in *"Image and vision computing"*, Vol. 15 (1), pp. 59-76.

[8] Sun, W., McBride, J-W., Hill, M., 2010. A new approach to characterizing aspheric surfaces, in *"Precision Engineering"*, Vol. 34(1), 2010, pp.171-179.

[9] Park, H., 2004. A solution for NURBS modelling in aspheric lens manufacture, in *"The Intl. J. of Adv.Manuf. Tech."*, Vol. 23 (1-2), pp.1-10.

[10] Forbes, A. B., 1993. Generalized regression problems in metrology. Numerical Algorithms, Vol. 5(10), pp. 523-533.

[11] Shakarji, C., 1998. Least-Squares fitting algorithms of the NIST algorithm testing system, in *"J. of research of the Nat. Inst. Of Std. and Tech."*, Vol. 103, pp. 633-641.

[12] Lancaster, P., 1966. Error analysis for the Newton-Raphson method, in *"Numerische Mathematik"*, Vol. 9 (1), pp. 55-68.

[13] Transtrum, M. K., & Sethna, J. P. (2012). Improvements to the Levenberg-Marquardt algorithm for nonlinear least-squares minimization.. arXiv preprint arXiv:1201.5885.

[14] Speer, T., Kuppe, M., Hoschek, J., 1998. Global reparametrization for curve approximation, in *"Computer Aided Geometric Design"*, Vol. 15 (9), pp. 869-877.

[15] Nocedal, J., 1980. Updating quasi-Newton matrices with limited storage, in *"Mathematics of computation"*, Vol. 35 (151), pp. 773-782.

[16] Liu, D., Nocedal, J., 1989. On the limited memory BFGS method for large scale optimization, in *"Mathematical programming"*, Vol. 45 (1-3), pp. 503-528.

[17] Zheng, W., Bo. P., Liu, Y., Wang, W., 2012. Fast B-Spline curve fitting by L-BFGS, in *"Computer Aided Geometric Design"*, Vol. 29 (7), pp. 448-462.

[18] El-Hayek, N., Nouira, H., Anwer, N., Damak, M., Gibaru, O., 2013. Reconstruction of freeform surfaces for metrology, in *"Proc. Of the 14th Intl. Conf. on Metrol. and Prop. of Eng. Surf."*, Vol. 1, pp. 36-47.

[19] Pomerlau, F., Colas, F., Siegwart, R., Magnenat, S., 2013. Comparing ICP variants on real-world data sets, in *"Autonomous Robots"*, Vol. 34 (3), pp. 133-148.

[20] Zhao, H., Anwer, N., Bourdet, P., 2013. Curvature-based Registration and Segmentation for Multisensor Coordinate Metrology, in *"Procedia CIRP"*, Vol. 10, pp. 112-118.

[21] Halina, N., Chuchro, Z., 2009. Some comments on reference data set generation in passing, in XIX IMEKO World Congress Fundamental and Applied Metrology, Lisbon, Portugal.

[22] Jiang, X., Zhang, X., Scott, P., 2010. Template matching of freeform surfaces based on orthogonal distance fitting for precision metrology, in *"Measurement Science and Technology"*, Vol. 21 (4), 10p.

[23] Mandelbrot, B., Ness, JW., 1968. Fractional Brownian Motions, Fractional Noise and applications, in *"SIAM Review"*, Vol.10, pp. 422–437.